RESEARCH PAPER

Ultrasonic Preparation of Cobalt, Nickel, Copper Ferrite Nanoparticles and Investigation of Mechanical Properties Ferrites Polymer Matrix Nanocomposites

Mohsen Hosseini [1], Hamidreza Rezaei Ashtiani [1*], Davood Ghanbari [2]

1 School of Mechanical Engineering, Arak University of Technology, Arak, Iran

[2] Department of Science, Arak University of Technology, Arak, Iran

ARTICLE INFO

Article History:
Received 19 March 2022
Accepted 13 June 2022
Published 01 July 2022

Keywords:
Ferrites nanoparticles
Mechanical properties
Polymer matrix nanocomposite
Ultrasonic method

ABSTRACT

In this study, cobalt, nickel, and copper ferrites nanoparticles were first synthesized using the ultrasonic method. In the next step, the nanoparticles were subjected to various analyzes such as X-ray diffraction pattern (XRD), scanning electron microscope (SEM), and infrared absorption spectroscopy (IR) to ensure their proper properties. In the next step, nanoparticles were added to the epoxy resin to make a polymer-based nanocomposite. Then, according to ASTM D638 standard, the samples were stretched and the results were compared with pure epoxy polymer. The results showed that the nanoparticles were made with a fine and uniform structure and high purity. The tensile test results showed that by adding these nanoparticles to the epoxy resin, the ultimate tensile strength (UTS) and the toughness of the nanocomposites improved compared to the epoxy polymer. The highest ultimate tensile strength was obtained in nanocomposites made of nickel ferrite nanoparticles whereas the highest toughness was obtained in nanocomposites made of copper ferrite nanoparticles.

How to cite this article
Hosseini M, Rezaei Ashtiani H, Ghanbari D. Ultrasonic Preparation of Cobalt, Nickel, Copper Ferrite Nanoparticles and Investigation of Mechanical Properties Ferrites Polymer Matrix Nanocomposites . J Nanostruct, 2022; 12(3):588-597. DOI: 10.22052/JNS.2022.03.012

INTRODUCTION

Ultrasonic is an eco-friendly, safe, and inexpensive technology[1,2] that is used as a versatile tool in a wide range of scientific and technological applications such as biology[3], chemistry[4], physics[5], medicine[6], materials science[7] and industrial applications[8–11]. One of the ultrasonic applications is the synthesis of nanoparticles[12]. The waves propagated in the aqueous solution form transient bubbles that explode, causing the nanostructures to disperse and form[13]. Epoxy resins are thermoset polymers that have interesting properties such as high chemical resistance, good tensile strength, compressive and flexural strength, good thermal resistance, and acceptable solubility[14–16] and then incorporated into PiP-DOPO through in situ reaction, resulting in the formation of the hybrids (PD-rGO. These polymers have received a lot of attention today due to their interesting properties and have many applications, including in the electronics, aerospace, and coating industries[17–19]. Xia et al [20] synthesized polyaniline nanoparticles using ultrasonic waves. They found that the use of ultrasonic waves increased the polymerization rate of aniline,

* *Corresponding Author Email: hr_rezaei@arakut.ac.ir*

which was very slow under normal conditions. Ultrasonic radiation also emits HCL molecules and improved the degree of doping. Song et al [21] synthesized magnesium hydroxide nanoparticles using the ultrasonic method. Their results showed that ultrasonic waves can limit the growth of magnesium hydroxide crystals in each lattice plate and improve the hydrophobicity of magnesium hydroxide nanoparticles. Rahmawati et al [22]400 and 400 kHz. The stirring rates performed in the synthesis process are varied from 500 to 900 rpm. The qualitative analysis by using X-Ray Diffractometer (XRD synthesized Fe_3O_4 nanoparticles using ultrasonic methods. Their results showed that using the deby sherer equation, the size of the Fe_3O_4 crystal from 21 to 25 nm depended on the ultrasonic frequency and the stirring speed. D. Gopi et al [23] synthesized hydroxyapatite nanoparticles by ultrasonic method. They investigated the time of ultrasonic irradiation on the size of nanoparticles in the presence of hollow spheres of glycine-acrylic acid. The results showed that the particle size decreases with increasing ultrasonic irradiation time. Therefore, the use of ultrasonic is an easy way to obtain nanoparticles, high quality anlppd with a suitable morphology. Mahdavi et al [24] investigated the effects of ultrasonic waves on the morphology and structure of ZnO nanoparticles. They observed that the purity of the samples increased with increasing ultrasonic wave power and irradiation time. Ultrasonic waves not only improve structure and morphology but also reduce grain size and prevent agglomeration. Alizadeh et al [25] used the ultrasonic method to synthesize CDs/TiO_2 nanoparticles. They used the response surface methodology to optimize the shell thickness and found that the strength of ultrasonic waves and time had the greatest effect on the nanoparticle size. Utara et al [26] synthesized barium titanate nanoparticles using ultrasonic at 25 ° C and atmospheric pressure without calcination. The results showed that a more uniform and regular structure formed with increasing ultrasonic time. Other researchers have synthesized ferritic and magnetic nanoparticles for various applications[27–31]. Lee et al. [32] fabricated a polymer-based composite using electrospinning technique and nanocarbon reinforcement and investigated its thermal, mechanical, and electrical properties. Hoon oh et al. [33]whether or not the reflective wave from an incident electromagnetic wave can be nullified. In this research, by blending conductive carbon black with the binder matrix of glass/epoxy composite, a radar absorbing structure (RAS constructed a radar-absorbing structure using glass/epoxy composite and carbon black in the X-band frequency range. Their system was designed to display the optimal amount of absorption for the X band in the range

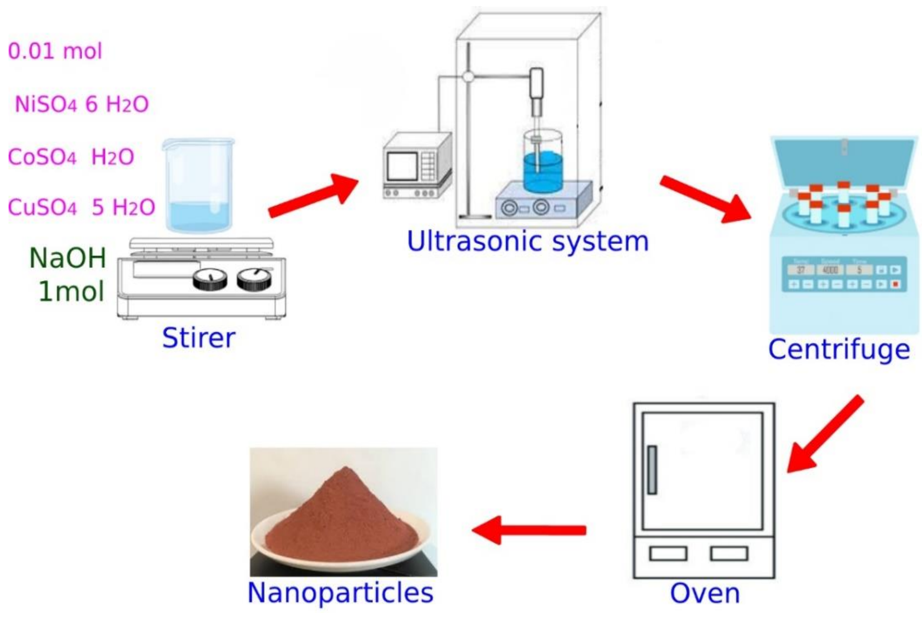

Fig. 1. Schematic of ultrasonic method for synthesis of nanoparticles.

of 8.2 to 12 GHz. ISA et al [34] investigated the effect of fiber type and its composition on the thermal, mechanical and physical properties of polyester composites. The results showed that the composite with Kevlar reinforcer has the highest tensile strength and the composite with handmade nylon fiber reinforcer has the lowest tensile strength. The composition of the fibers also improved the thermal properties of the composite and had a positive effect on water absorption and density. Xu Ma et al [35] worked on the synthesis of degradable hyper branched epoxy resin and found that not only simultaneously elongation, tensile properties, modulus, flexural strength and impact resistance were increased about 50%, 64.8%, 70.4%, 38.1% and 93.7% respectively, but also their low temperature resistance improves.

In this paper, nanoparticles were first fabricated using the ultrasonic method as green and ecofriendly method and their properties were investigated. These nanoparticles were then added to the epoxy resin and the mechanical properties consist of ultimate tensile strength and toughness of the nanocomposites were investigated and compared with each other and epoxy polymer.

MATERIALS AND METHODS

To produce nanoparticles by ultrasonic method, first 0.97 g of iron nitrate per 0.3 g of cobalt sulfate, 0.92 g of iron nitrate per 0.3 g of nickel sulfate, and 1.2 g of iron nitrate per 0.3 g of copper sulfate were poured into 150 ml of distilled water and mixed with a stirrer for 20 minutes. The solution was then immersed in an ultrasonic device for 20 minutes. While the solution was in the ultrasonic device, 1 molar sodium hydroxide solution was slowly added to the main solution to bring the pH to 11. In the next step, the solution was centrifuged and placed in the oven to dry the nanoparticles and be ready for use in the next steps. Fig. 2 shows a schematic of the ultrasonic method.

To produce the polymer matrix composite, 5% by weight of the nanoparticles were first added to the epoxy resin and mixed together for 20 minutes. The produced composites were then placed in a vacuum apparatus for 20 minutes and placed in a room for two hours to de-bubble and eliminate pores. In the next step, the composites were poured into the mold and placed according to the standard at room temperature and then in the furnace to find the necessary mechanical properties. To evaluate the mechanical properties of the samples, nanocomposites made with a thickness of 4 mm according to the ASTM D638 standard and at a speed of 0.5 mm/min were tested. All tests were repeated three times and their mean was reported.

RESULTS AND DISCUSSION

To identify the phase, XRD analysis was taken from the generated samples, which is shown in Figs. 2-4. Fig. 2 illustrates the X-ray diffraction pattern (XRD) of cobalt ferrite nanoparticles

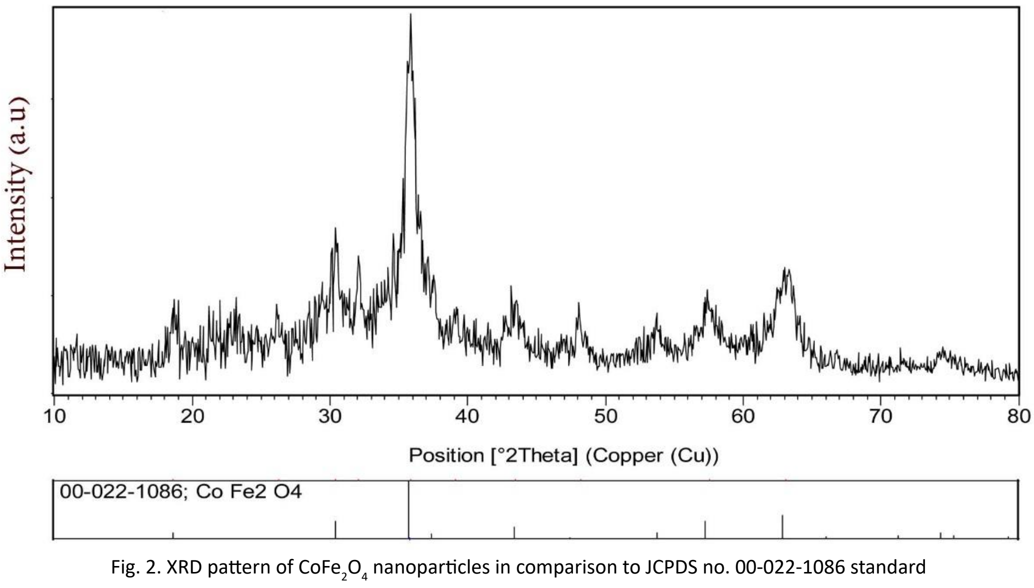

Fig. 2. XRD pattern of $CoFe_2O_4$ nanoparticles in comparison to JCPDS no. 00-022-1086 standard

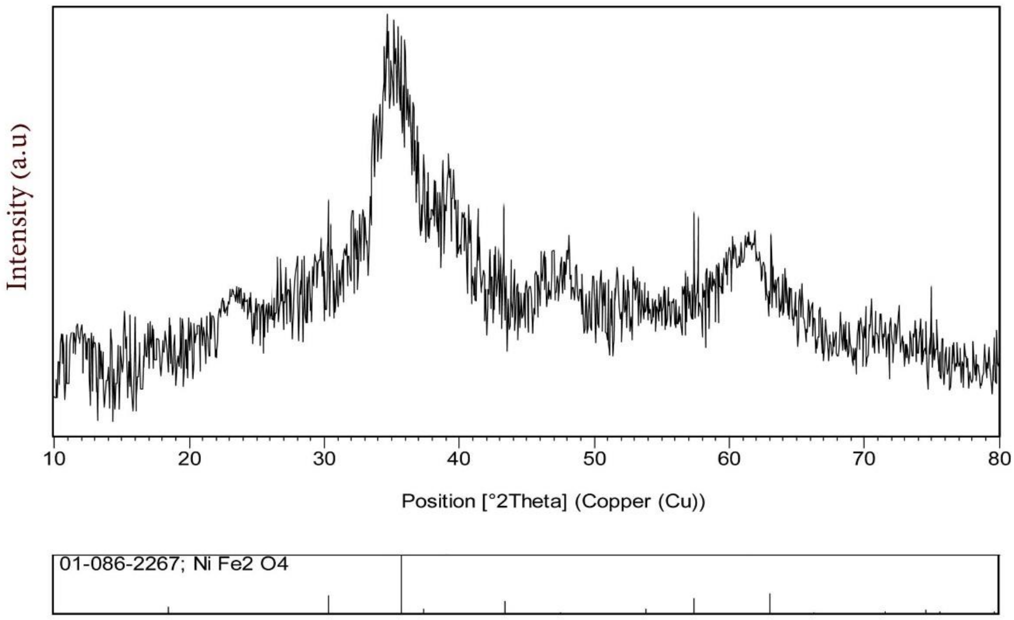

Fig. 3. XRD pattern of fabricated $NiFe_2O_4$ nanoparticles in comparison to JCPDS 01-086-2267 standard.

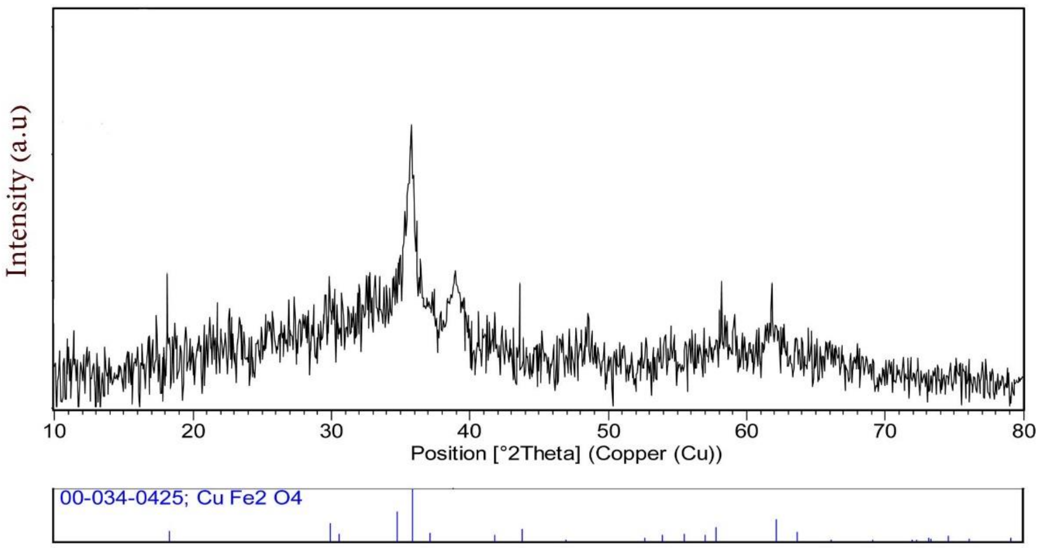

Fig. 4. XRD pattern of $CuFe_2O_4$ nanoparticles in comparison to JCPDS no. 00-034-0425 standard.

($CoFe_2O_4$) nanoparticles, the pattern has a suitable agreement with pure material standard using JCPDS: 00-022-1086 and Miller indexes include (220), (311), (400), (422), (511), (440) are observed in the pattern and approve purity of the phase in this rapid and simple reaction. XRD pattern of nickel ferrite nanoparticles ($NiFe_2O_4$) is shown in Fig. 3, also this spectrum has appropriate accordance with pure standard using JCPDS: 01-086-2267 and by miller indexes: (220), (311), (222), (400), (422), (440), (622), (444). Fig. 4 depicts the XRD pattern of copper ferrite nanoparticle (CuFe2O4) with JCPDS: 00-034-0425 and by miller indexes: (202), (311), (004), (224), (333), and (440).

An electron scan microscope was used to evaluate the morphology and particle size, with

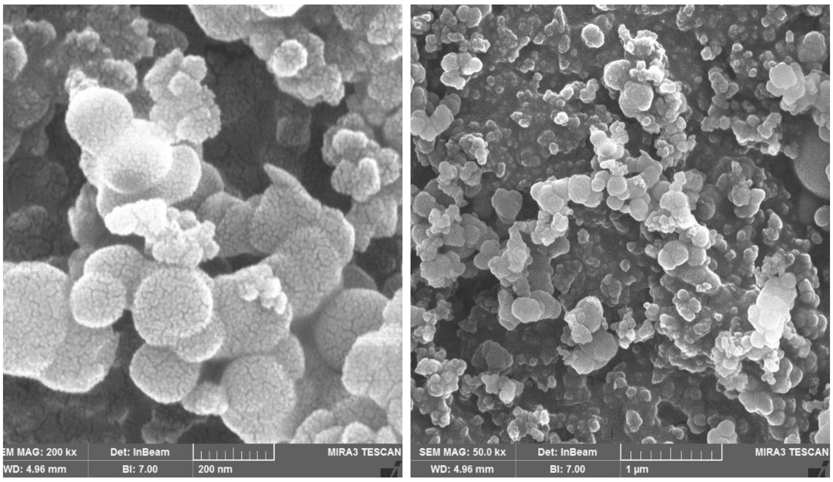

Fig. 5. SEM images of $CoFe_2O_4$ nanoparticles synthesized by ultrasonic method.

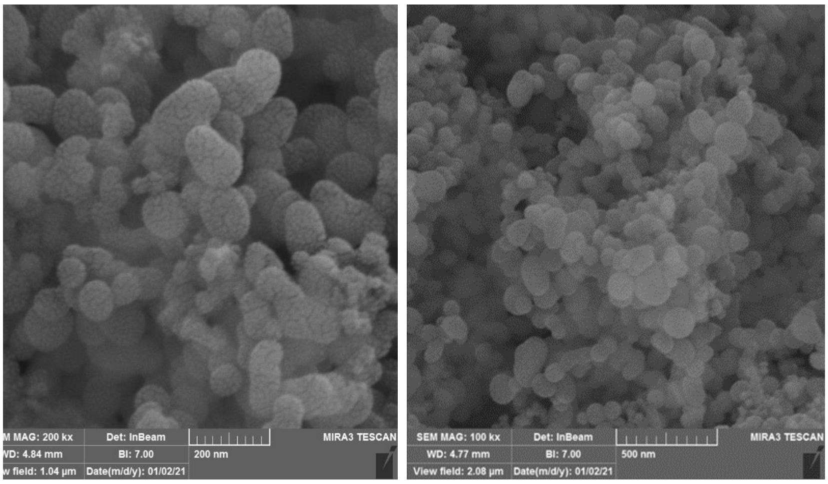

Fig. 6. SEM images of $NiFe_2O_4$ nanoparticles synthesized by ultrasonic method.

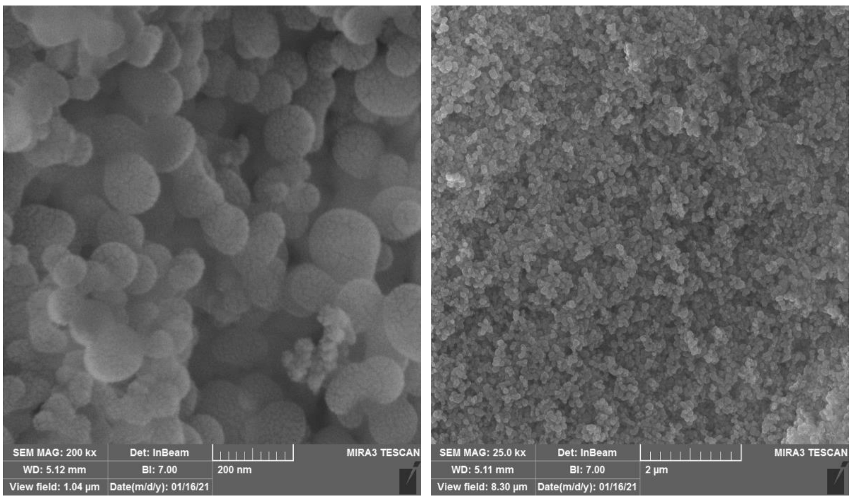

Fig. 7. SEM images of $CuFe_2O_4$ nanoparticles synthesized by ultrasonic method.

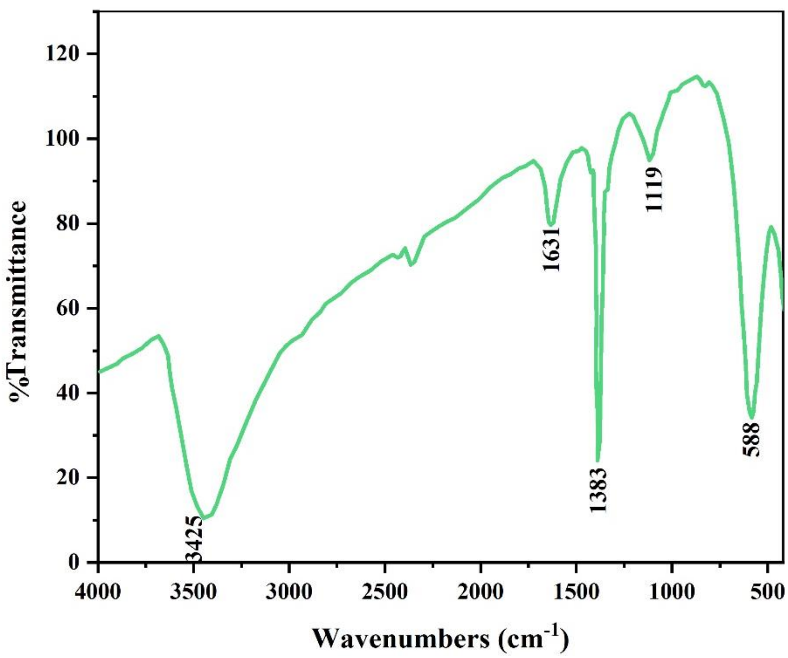

Fig. 8. Infrared absorption spectroscopy of $CoFe_2O_4$ nanoparticles.

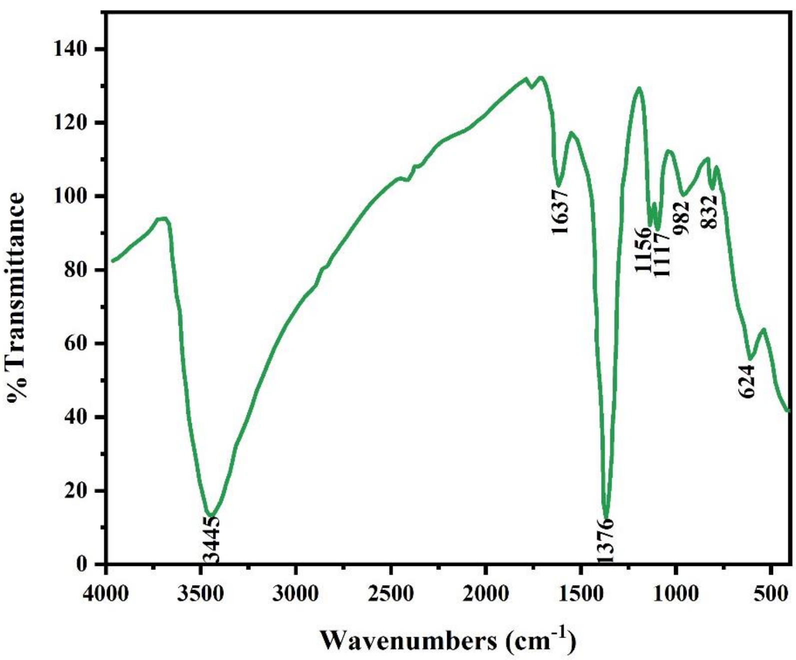

Fig. 9. Infrared absorption spectroscopy of $NiFe_2O_4$ nanoparticles.

different magnifications showing Figs. 5 to 7. Fig 5 shows an electron scanning microscope image of cobalt ferrite nanoparticles with different magnifications and a work distance of 4.96 mm. Fig. 6 shows an electron scanning microscope image of nickel ferrite nanoparticles. The images confirm the formation of nanoparticles with a fine and uniform structure. Scanning electron microscope images with magnifications of 100 and 200 kx and work distances of 4.77 and 4.84 mm and at scales of 200 and 500 nm of copper ferrite nanoparticles are also shown in Fig. 7.

Figs. 8 to10 show the infrared absorption spectroscopy of cobalt ferrite, nickel ferrite, and copper ferrite nanoparticles. Peaks in areas 588, 624, and 438 related to metal-oxygen bonding,

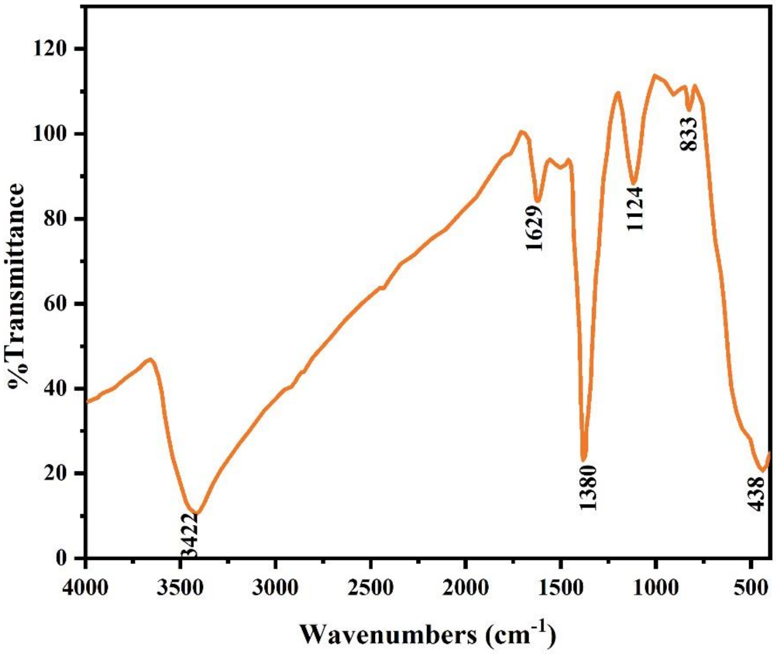

Fig. 10. Infrared absorption spectroscopy of $CuFe_2O_4$ nanoparticles.

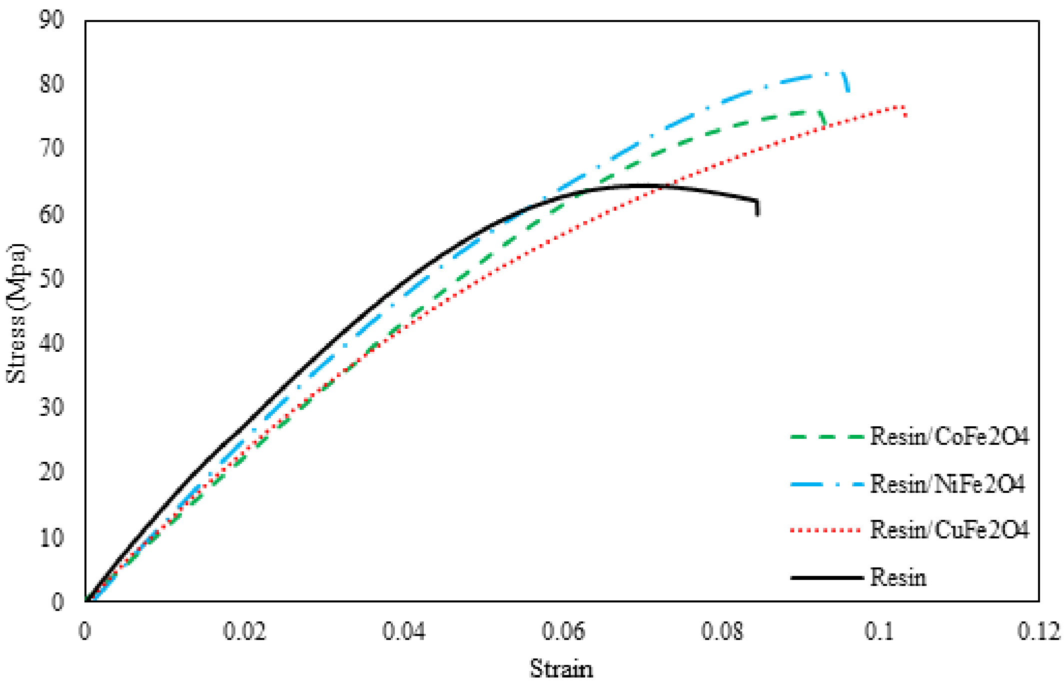

Fig. 11. Stress-strain diagrams of the different nanocomposites and the base resin polymer.

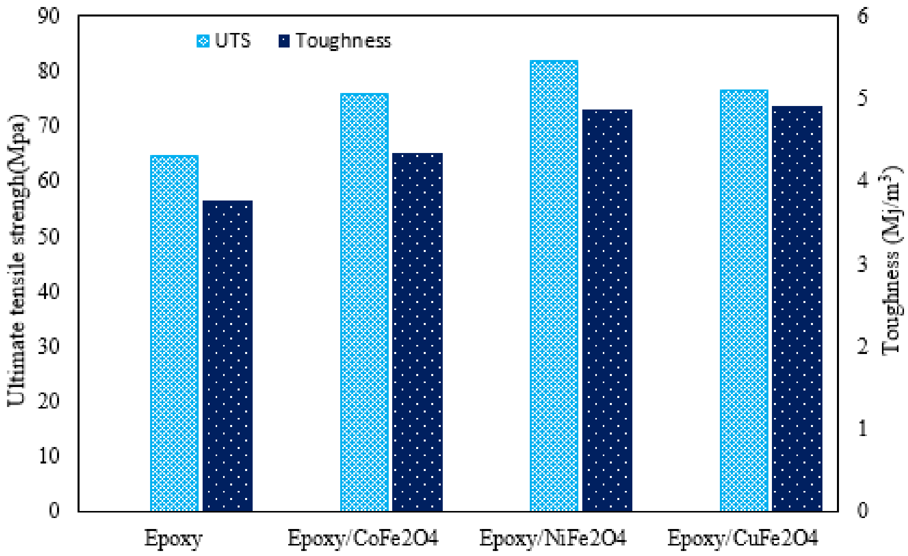

Fig. 12. Comparison of ultimate tensile strength and toughness of different nanocomposites and base epoxy polymer.

peaks in areas 1119-1631, 1117-1537, and 1124-1629 related to synthetic precursors, and wide peaks in areas 3425, 3445, and 3422 related to oxygen-hydrogen bonding.

Fig. 11 shows the stress-strain diagrams of the composites and the base polymer. As can be seen, after adding nanoparticles to the epoxy resin and their uniform distribution, the final tensile strength of the composites has significantly improved compared to the base polymer, which can be due to the homogeneous distribution of nanoparticles in the matrix of epoxy resin and adhesion between epoxy resin and nanoparticles[36]. Also, by adding nanoparticles to the epoxy resin, the toughness of the composite has improved compared to the base polymer. The UTS and toughness values are 75.93539 MPa and 4.326422 Mj/m^3 for epoxy/$CoFe_2O_4$ nanocomposite, 81.79603 MPa and 4.861615 Mj/m^3 for epoxy/$NiFe_2O_4$ nanocomposite, 76.6423 MPa and 4.91496 Mj/m^3 for epoxy/$CuFe_2O_4$ composite, and 64.43333 MPa and 3.76838 Mj/m^3 for pure polymer, respectively. The highest ultimate tensile strength was observed in epoxy/$NiFe_2O_4$ nanocomposite and the lowest ultimate tensile strength was observed in the pure epoxy polymer. Also, the highest toughness was observed in epoxy/$CuFe_2O_4$ composite and the lowest toughness was observed in the pure epoxy polymer. The changes of which are shown in Fig. 12. Also, the highest ultimate tensile strength was observed in the nanocomposite fabricated with nickel ferrite nanoparticles.

CONCLUSIONS

In this paper, different ferrite nanoparticles were first produced in a very simple, inexpensive, and practical method and their properties were investigated. Then nanocomposites were produced with these nanoparticles and their tensile properties were investigated. Based on the results of this paper, ultrasonic is a suitable method for the production of nanoparticles with a uniform and fine-grained structure, and the nanoparticles produced to comply with standard peaks. According to the results of the tensile test of the samples, the composites produced, in addition to better ultimate tensile strength than the base polymer, also have better toughness. The highest ultimate tensile strength was obtained in nanocomposites fabricated with nickel ferrite nanoparticles and the highest toughness value was obtained in nanocomposites made of copper ferrite nanoparticles.

CONFLICT OF INTEREST

The authors declare that there is no conflict of interests regarding the publication of this manuscript.

REFERENCES

1. Wang J, Fan J, Li J, Wu X, Zhang G. Ultrasound assisted synthesis of Bi2NbO5F/rectorite composite and its

photocatalytic mechanism insights. Ultrason Sonochem. 2018;48:404-411.
2. Alipanahpour Dil E, Ghaedi M, Asfaram A, Zare F, Mehrabi F, Sadeghfar F. Comparison between dispersive solid-phase and dispersive liquid–liquid microextraction combined with spectrophotometric determination of malachite green in water samples based on ultrasound-assisted and preconcentration under multi-variable experimental design optimization. Ultrason Sonochem. 2017;39:374-383.
3. Theerdhala S, Bahadur D, Vitta S, Perkas N, Zhong Z, Gedanken A. Sonochemical stabilization of ultrafine colloidal biocompatible magnetite nanoparticles using amino acid, l-arginine, for possible bio applications. Ultrason Sonochem. 2010;17(4):730-737.
4. Doktycz SJ, Suslick KS. Interparticle Collisions Driven by Ultrasound. Science. 1990;247(4946):1067-1069.
5. Egerton RF. Limits to the spatial, energy and momentum resolution of electron energy-loss spectroscopy. Ultramicroscopy. 2007;107(8):575-586.
6. Handbook on Applications of Ultrasound. CRC Press; 2011.
7. Mason T, Peters D. An introduction to the uses of power ultrasound in chemistry. Practical Sonochemistry: Elsevier; 2002. p. 1-48.
8. Vilkhu K, Mawson R, Simons L, Bates D. Applications and opportunities for ultrasound assisted extraction in the food industry — A review. Innovative Food Science & Emerging Technologies. 2008;9(2):161-169.
9. Bazrafshan AA, Ghaedi M, Hajati S, Naghiha R, Asfaram A. Synthesis of ZnO-nanorod-based materials for antibacterial, antifungal activities, DNA cleavage and efficient ultrasound-assisted dyes adsorption. Ecotoxicology and Environmental Safety. 2017;142:330-337.
10. Asfaram A, Ghaedi M, Purkait MK. Novel synthesis of nanocomposite for the extraction of Sildenafil Citrate (Viagra) from water and urine samples: Process screening and optimization. Ultrason Sonochem. 2017;38:463-472.
11. Khafri HZ, Ghaedi M, Asfaram A, Safarpoor M. Synthesis and characterization of ZnS:Ni-NPs loaded on AC derived from apple tree wood and their applicability for the ultrasound assisted comparative adsorption of cationic dyes based on the experimental design. Ultrason Sonochem. 2017;38:371-380.
12. Gedanken A. Using sonochemistry for the fabrication of nanomaterials. Ultrason Sonochem. 2004;11(2):47-55.
13. Barcikowski S, Plech A, Suslick KS, Vogel A. Materials synthesis in a bubble. MRS Bulletin. 2019;44(5):382-391.
14. Guo W, Yu B, Yuan Y, Song L, Hu Y. In situ preparation of reduced graphene oxide/DOPO-based phosphonamidate hybrids towards high-performance epoxy nanocomposites. Composites Part B: Engineering. 2017;123:154-164.
15. Qiu S, Zhou Y, Zhou X, Zhang T, Wang C, Yuen RKK, et al. Air-Stable Polyphosphazene-Functionalized Few-Layer Black Phosphorene for Flame Retardancy of Epoxy Resins. Small. 2019;15(10):1805175.
16. Wang X, Chen T, Hong J, Luo W, Zeng B, Yuan C, et al. In-situ growth of metal-organophosphorus nanosheet/nanorod on graphene for enhancing flame retardancy and mechanical properties of epoxy resin. Composites Part B: Engineering. 2020;200:108271.
17. Han J, Liang G, Gu A, Ye J, Zhang Z, Yuan L. A novel inorganic–organic hybridized intumescent flame retardant and its super flame retarding cyanate ester resins. J Mater Chem A. 2013;1(6):2169-2182.
18. Zhou H, Chen R, Liu Q, Liu J, Yu J, Wang C, et al. Fabrication of ZnO/epoxy resin superhydrophobic coating on AZ31 magnesium alloy. Chem Eng J. 2019;368:261-272.
19. Li X-L, Zhang F-H, Jian R-K, Ai Y-F, Ma J-L, Hui G-J, et al. Influence of eco-friendly calcium gluconate on the intumescent flame-retardant epoxy resin: Flame retardancy, smoke suppression and mechanical properties. Composites Part B: Engineering. 2019;176:107200.
20. Zhang Z, Wang XL, Xu J, Ma HC, Lei ZQ. Ultrasonic Assisted Dynamic Inverse Emulsion: A Novel Polymerization Technique to Prepare Conductive Polyaniline/Palygorskite Composite. Advanced Materials Research. 2013;873:507-513.
21. Song G, Ma S, Tang G, Wang X. Ultrasonic-assisted synthesis of hydrophobic magnesium hydroxide nanoparticles. Colloids Surf Physicochem Eng Aspects. 2010;364(1-3):99-104.
22. Rahmawati R, Permana MG, Harison B, Nugraha, Yuliarto B, Suyatman, et al. Optimization of Frequency and Stirring Rate for Synthesis of Magnetite (Fe_3O_4) Nanoparticles by Using Coprecipitation- Ultrasonic Irradiation Methods. Procedia Engineering. 2017;170:55-59.
23. Gopi D, Indira J, Kavitha L, Sekar M, Mudali UK. Synthesis of hydroxyapatite nanoparticles by a novel ultrasonic assisted with mixed hollow sphere template method. Spectrochimica Acta Part A: Molecular and Biomolecular Spectroscopy. 2012;93:131-134.
24. Abdulrazzaq Naji, S., Al-azzawi, M. Effect of Zirconium Oxide -Titanium Dioxide Nanoparticles on Mechanical and Physical Properties of Soft Denture Lining Materials. Journal of Nanostructures, 2022; 12(1): 34-44.
25. Alizadeh S, Fallah N, Nikazar M. An ultrasonic method for the synthesis, control and optimization of CdS/TiO_2 core-shell nanocomposites. RSC advances. 2019;9(8):4314-4324.
26. Utara S, Hunpratub S. Ultrasonic assisted synthesis of $BaTiO_3$ nanoparticles at 25 °C and atmospheric pressure. Ultrason Sonochem. 2018;41:441-448.
27. Ahmadian-Fard-Fini S, Ghanbari D, Salavati-Niasari M. Photoluminescence carbon dot as a sensor for detecting of Pseudomonas aeruginosa bacteria: Hydrothermal synthesis of magnetic hollow $NiFe_2O_4$-carbon dots nanocomposite material. Composites Part B: Engineering. 2019;161:564-577.
28. Ahmadian-Fard-Fini S, Salavati-Niasari M, Ghanbari D. Hydrothermal green synthesis of magnetic Fe_3O_4-carbon dots by lemon and grape fruit extracts and as a photoluminescence sensor for detecting of E. coli bacteria. Spectrochimica Acta Part A: Molecular and Biomolecular Spectroscopy. 2018;203:481-493.
29. Etminan M, Nabiyouni G, Ghanbari D. Preparation of tin ferrite–tin oxide by hydrothermal, precipitation and auto-combustion: photo-catalyst and magnetic nanocomposites for degradation of toxic azo-dyes. Journal of Materials Science: Materials in Electronics. 2017;29(3):1766-1776.
30. Ahmadian-Fard-Fini S, Ghanbari D, Amiri O, Salavati-Niasari M. Electro-spinning of cellulose acetate nanofibers/Fe/carbon dot as photoluminescence sensor for mercury (II) and lead (II) ions. Carbohydr Polym. 2020;229:115428.
31. Lee JKY, Chen N, Peng S, Li L, Tian L, Thakor N, et al. Polymer-based composites by electrospinning: Preparation & functionalization with nanocarbons. Prog Polym Sci. 2018;86:40-84.
32. Oh J-H, Oh K-S, Kim C-G, Hong C-S. Design of radar absorbing

structures using glass/epoxy composite containing carbon black in X-band frequency ranges. Composites Part B: Engineering. 2004;35(1):49-56.
33. Isa MT, Ahmed AS, Aderemi BO, Taib RM, Mohammed-Dabo IA. Effect of fiber type and combinations on the mechanical, physical and thermal stability properties of polyester hybrid composites. Composites Part B: Engineering. 2013;52:217-223.
34. Ma X, Guo W, Xu Z, Chen S, Cheng J, Zhang J, et al. Synthesis of degradable hyperbranched epoxy resins with high tensile, elongation, modulus and low-temperature resistance. Composites Part B: Engineering. 2020;192:108005.
35. Ma X, Peng C, Zhou D, Wu Z, Li S, Wang J, et al. Synthesis and mechanical properties of the epoxy resin composites filled with sol–gel derived ZrO_2 nanoparticles. Journal of Sol-Gel Science and Technology. 2018;88(2):442-453.
36. Tavakoli H. Thermal Decomposition of Ammonium Perchlorate in the Presence of Functionalized MWCNTs. Journal of Nanostructures. 2022;12(2):235-244.